Cellulose
https://doi.org/10.1007/s10570-018-1729-z

ORIGINAL PAPER

Bilayer biocomposites based on coated cellulose paperboard with films of polyhydroxybutyrate/cellulose nanocrystals

I. T. Seoane · L. B. Manfredi · V. P. Cyras

Received: 18 October 2017 / Accepted: 26 February 2018

Abstract In this paper, a biodegradable bilayer nanocomposite based on reinforced polyhydroxybutyrate (PHB) with cellulose nanocrystals (CNC) and cellulose paperboard was prepared. In order to obtain optimal properties two different processing methods were studied: casting and compression molding. Compression molding was selected as the most effective technique to achieve a continuous layer of PHB covering the entire surface of the paperboard. Mechanical and barrier properties of the composites were optimized, using the least amount of PHB due to its high cost compared to fossil-derived polymers. Then, the bilayer nanocomposite was produced according to the selected method and the least PHB proportion, demonstrating that PHB/CNC coating overcomes water sensibility of the cellulose paperboard and exhibited a performance enhancement without detrimental effect of the pristine PHB and paperboard properties. It was demonstrated that PHB and PHB/CNC have the potential to replace non-renewable polymers as fully bio-based materials, obtaining paperboard coatings with environmental advantages, such as non-toxicity, high recyclability and biodegradability.

I. T. Seoane · L. B. Manfredi · V. P. Cyras (✉)
Instituto de Investigaciones en Ciencia y Tecnología de Materiales (INTEMA), UNMdP, CONICET, Facultad de Ingeniería, Av. Juan B Justo 4302,
B7608FDQ Mar del Plata, Argentina
e-mail: vpcyras@fi.mdp.edu.ar

Keywords Poly(3-hydroxybutyrate) · Cellulose paperboard, Cellulose nanocrystals · Bilayer biocomposite

Introduction

Cellulose paperboard packaging presents high demand on the market since its use provides high recycling rates, ensuring greater sustainability advantages (Farmer 2013). In particular, sisal is one of the natural fibers widely available in most parts of the world (Saxena et al. 2011). In general, the agrobased biopolymers are edible, biocompatible and biodegradable, which make them superior to synthetic polymers and particularly useful in disposable plastics and food (Farmer 2013). However, the low water vapor barrier capacity of cellulose paperboard is considered a limitation for their use in packaging (Siracusa et al. 2008). Therefore, different polymeric materials used as coatings, such as polyethylene, polyvinyl alcohol or natural wax were developed (Peelman et al. 2013; Robertson 2013). Additionally, the use of a protective polymeric film gives mechanical integrity and can improve the effectiveness of the heat sealing (Kontominas 2010).

Most of the synthetic polymers are produced from petrochemicals and these materials are not easily degradable, causing environmental problems. In recent years, research has been focusing to replace

Published online: 01 March 2018

fossil or non-degradable raw materials with biodegradable or recyclable materials in the manufacture of paperboard laminates. Renewable or biodegradable polymers proved to be potential barrier coatings, replacing current synthetic ones (Rastogi and Samyn 2015). Starch and cellulose derivatives, chitosan, alginate, wheat gluten, whey proteins, polycaprolactone, poly(lactic acid) and polyhydroxyalkanoates (PHAs) are among the most widely used biodegradable polymers (Andersson 2008). At present, the demand for packaging has evolved into smaller and lighter ones. Also, recoverability and recyclability are required features for environmental and economic reasons. This is why coating of biopolymers on paperboard products could fill this need, presenting biodegradable added value, as long as processing technology is developed and energy consumption is reduced (Johansson et al. 2012).

PHAs are polyesters biosynthesized by microorganisms. Polyhydroxybutyrate (PHB) is the most common PHA due to its good biodegradability and biocompatibility. Moreover, PHB has stereochemical regularity and their chains are completely linear, which allow its high crystallinity degree, around 60%. Therefore, its crystallinity and hydrophobicity contribute to present significant barrier properties (Plackett and Vázquez 2004). PHB presents water vapor barrier properties in the range of other synthetic conventional thermoplastics, such as polyethylene terephthalate, low-density polyethylene and polyvinyl alcohol (Arrieta et al. 2017; Desobry and Arab-Tehrany 2014). Another advantage is that it can be extruded or molded using conventional processing equipment, so it appears as a good candidate for producing biodegradable products like bottles, bags, films, etc. (Mekonnen et al. 2013).

The use of a thin film of PHB could protect cellulose paperboard. In this manner, a low cost and biodegradable composite is obtained. PHB has been used as a paperboard coating, presenting final properties that depend on the processing method (Seoane et al. 2015). The use of a thin layer of PHB by casting, using chloroform as solvent, reduces the absorption of moisture and water, water vapor permeation and surface roughness, as well as improves mechanical properties of the cellulose paperboard (Cyras et al. 2007). Also, the application of PHB by compression molding presents the greatest increase of barrier and mechanical properties, with an additional improvement when the paperboard is chemically modified to have a better adhesion with the coating (Cyras et al. 2009).

In order to obtain a multilayer composite with good mechanical properties, it is essential to ensure good adhesion between the polymeric coating and the paperboard. As occurs in natural fiber-reinforced composites, the load is transferred between the matrix and the fibers through shear stresses at the interface (Njuguna et al. 2011; Puglia et al. 2016). One way to improve adhesion is the compatibilization of the materials through chemical treatments or the addition of compatible particles (Cyras et al. 2009). Poor adhesion results in detrimental effects on the mechanical properties and the increase of the vulnerability to the environmental attack. Nanotechnology is able to improve the behavior of biopolymers and give additional water resistance (Rastogi and Samyn 2015). The use of cellulose nanocrystals (CNC) as matrix nanofiller can provide specific barrier properties to gases and oil as well as good mechanical properties as observed in PHBV-based nanocomposites (Yu et al. 2014). Furthermore, the inclusion of hydrophilic nanoparticles into the hydrophobic PHB matrix could improve the nanocomposite compatibility with the paperboard, increasing the adhesion between them.

The purpose of this work is to obtain fully biodegradable bilayer composites with cellulose paperboard and reinforced PHB to be used in packaging. First, two manufacturing techniques (casting and compression molding) were considered. Barrier and mechanical properties were evaluated as a function of PHB coating weight, in order to choose the processing technique and the PHB/cardboard ratio that achieve the optimal final properties. In a second part, cellulose nanoparticles were added into the PHB layer, to improve the thermal, mechanical and barrier properties of the bilayer material as well as the adhesion between the layers.

Experimental

Materials

Polyhydroxybutyrate (PHB), with an average molecular weight (Mw) of 600,000 g/mol, was kindly supplied by Biocycle®. PHB is produced during

fermentation of saccharose in sugarcane by natural microorganisms of *Alcaligene genus*.

Cellulose paperboard of sisal was from Celesa Celulosa of Levante S.A.. Microcrystalline cellulose (MCC, dimensions of 10–15 μm) was supplied by Sigma-Aldrich (St. Louis, MO, USA). *N,N*-Dimethylformamide (DMF) and sulphuric acid were from Cicarelli Laboratories.

Methods

Preparation of bilayer composites by casting

Homogeneous solutions with different amounts of PHB (5, 10, 15 and 20 wt% of PHB/paperboard ratio) in DMF were prepared by stirring at 116 °C to ensure total dissolution. These solutions were poured onto cellulose paperboard in Petri dishes and kept in an oven at 80 °C for 12 h to eliminate solvent by evaporation. The films were stored at room temperature for 15 days to complete PHB crystallization.

Preparation of bilayer composites by compression molding

Biocomposites were obtained by pressing a film of PHB and cellulose paperboard at 70 kg/cm^2 and 160 °C. Different percentages of PHB (5, 10, 15 and 20 wt%) were used related to a paperboard weight of ca. 4.7 g. Dried films were stored at room temperature for 15 days in order to allow the complete crystallization of PHB.

Preparation of cellulose nanoparticles

Cellulose nanocrystals (CNC) were obtained by hydrolysis of MCC in sulphuric acid (64 wt%) at 45 °C for 40 min following the recipe used by Morán et al. (2008). Following the hydrolysis, the suspension was immediately diluted with bi-distilled water to quench the reaction and then, the suspension was dialyzed against water for 10 days. An ultrasonic treatment was performed by means of a tip sonicator (Cole Parmer) for 4 times of 5 min. Finally, CNC were freeze dried by a VirTis benchtop SLC lyophilizer. The obtained CNC showed the typical dimensions ranging from 130 to 290 nm in length and 3–6 nm in width.

A sample of PHB was reinforced with 4 wt% of CNC. This percentage was selected in order to reduce water vapor permeability, maintaining flexibility, considering a previous work (Seoane et al. 2017). This CNC amount was previously ultrasonicated in DMF and then, added to the PHB dissolution. Then, the mix was ultrasonicated and dried in an oven at 80 °C for 12 h.

Structural and thermal characterization

Fourier transform infrared (FTIR) spectroscopy was performed on the upper and lower faces of the composites to study the chemical structure of both film sides. The spectra were acquired with a Mattson Genesis II spectrometer, with a spectral width of 400–4000 cm^{-1}, 32 accumulations, 4 cm^{-1} resolution, in DRIFT mode. In order to compare spectra of different samples, each spectrum was normalized to the band at 2900 cm^{-1}. This band corresponds to the stretching of CH_2 groups; which is insensitive to the composition and degree of crystallinity (Cyras et al. 2009).

The composites surfaces were coated with a 300 Å gold layer and their morphologies were analyzed by means of scanning electron microscopy (SEM) in a JEOL JSM-6460LV equipment and field emission scanning electron microscopy (FE-SEM) using a Carl Zeiss NTS SUPRA 40 SEM microscope.

Differential scanning calorimetry (DSC) analyses were carried out using a Perkin Elmer DSC instrument under nitrogen atmosphere. Heating run was made from ambient temperature to 195 °C, at a rate of 10 °C/min, to determine melting temperature (T_m) and crystallinity degree (Xc). Xc can be determined using the following equation, as a function of melting peaks area:

$$\mathrm{Xc}(\%) = \frac{\Delta H_m}{\Delta H_m^0 \cdot w_{PHB}} \times 100 \quad (1)$$

where ΔH_m is PHB melting enthalpy, ΔH_m^0 is the melting heat associated with pure crystalline PHB (146 J/g) (Barham et al. 1984) and w_{PHB} is the weight fraction of PHB in the composite.

Thermogravimetric Analyses (TGA) were performed using a TA instruments Auto-MTGA Q500 Hi-Res thermogravimetric analyzer. Temperature program was run from 25 to 700 °C at a 10 °C/min

heating rate under nitrogen atmosphere (30 mL/min) in order to prevent any thermo-oxidative reaction. The sample weight in all tests was approximately 10 mg.

X-ray diffraction (XRD) measurements were obtained with KCuα (λ = 1.54 Å) radiation in a Philips PW 1710 X-ray diffractometer system. The X-ray tube was operated at 45 kV and 30 mA, at 2°/min in the 2θ range from 5° to 60°.

Mechanical characterization

Mechanical properties of the composites were determined with the INSTRON 4467 mechanical testing machine. Tensile testing of bone-shaped composite specimens was carried out using a crosshead rate of 1 mm/min (ASTM D 638-03).

Water vapor permeability

Water vapor permeability (WVP) tests were conducted in accordance with ASTM E 96-80 method 17. Each film sample was sealed over a circular opening of 0.00177 m^2 in a permeation cell that was stored at 20 °C and 64.5% of relative humidity (RH) in a controlled chamber. To maintain the highest gradient across the film, anhydrous $CaCl_2$ (0% RH) was placed inside the cell. The RH inside the cell was always lower than that outside, and water vapor transport was determined from the weight gain of the permeation cell. When steady state conditions were reached (about 1 day), weight measurements were made over 10 days. Changes in the weight of the cell were recorded as a function of time with all the samples. At least three repetitions per experiment were performed.

Water vapor transmission rate (WVTR) is a weight gain and was calculated as the relation between the slope of each curve of weight versus time (g/s), determined by linear regression, and the cell area (m^2). Permeability was then calculated according to the following equation:

$$WVP\left(\frac{g}{s \cdot m \cdot Pa}\right) = \frac{WVTR}{S \cdot (R2 - R1)} \cdot d \qquad (2)$$

where S is vapor pressure of water at saturation (Pa) at test temperature (20 °C), R1 is RH inside the permeation cell (R1 = 0), R2 is RH in the chamber (R2 = 64.5%) and d is film thickness (m). Each WVP reported was the mean value of at least six samples.

Results and discussion

Bilayer composites of PHB and paperboard

Bilayer composites were obtained by two processing techniques, casting and compression molding. The samples were prepared with different PHB contents based on paperboard weight (5, 10, 15 and 20 wt%). First, all obtained composites were characterized in order to select the processing technique and the weight relation PHB/paperboard that allow obtaining a composite with adequate properties to be used in packaging.

Chemical structure of bilayer composites was characterized by FTIR, Fig. 1. The infrared spectra

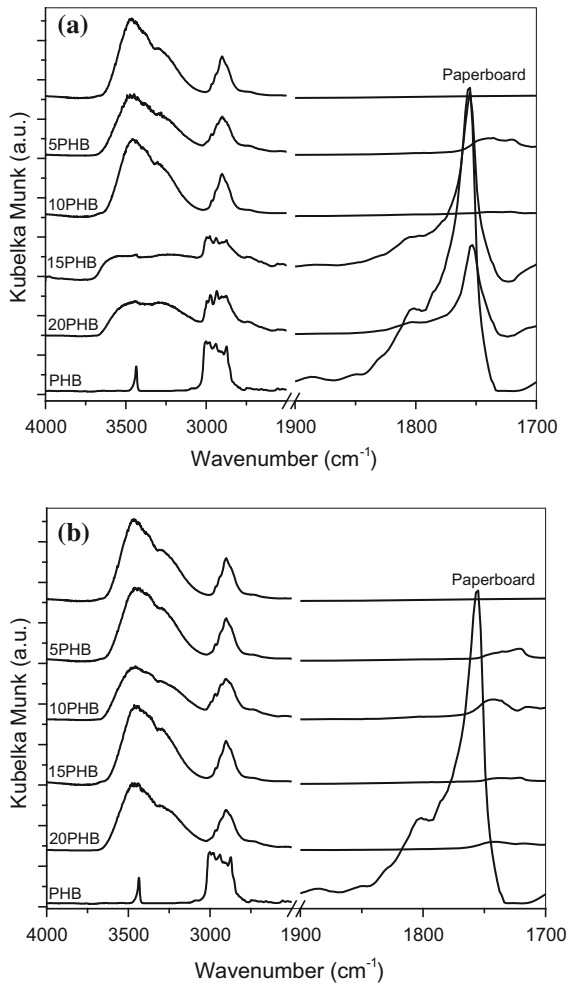

Fig. 1 Normalized FTIR spectra (DRIFT) of **a** upper face and **b** lower face of bilayer composites with different coating percentage obtained by casting

of both sides of the samples were carried out. The side where PHB had been poured was identified by "upper face" and the other, as "lower face". Native paperboard and a film of neat PHB prepared by casting were also studied. Figure 1a and b show the upper and lower faces, respectively, of the bilayer composites spectra with different PHB percentages. In Fig. 1a, it was observed that the spectra of composites with low PHB contents resulted similar to the one of the paperboard, with a slight reduction of superficial hydroxyl group absorbance (band at the zone 3400–3600 cm^{-1}). At the same time, the spectra of the bilayers with 15 and 20 wt% of PHB presented the characteristic peaks of PHB, as the band 1755 cm^{-1} corresponding to carbonyl group which did not appear at paperboard spectrum (D'Amico et al. 2012). Then, 15 wt% of PHB was found to be sufficient to almost cover the entire paper surface. Furthermore, characteristic PHB peaks did not appear in the spectra of the lower face of bilayer composites (Fig. 1b). Therefore, it seems that a portion of PHB diffused through paperboard fibers without reaching the opposite side of the composite, including high coat weight as 15 and 20 wt%. These results were corroborated by SEM. Figure 2 shows the micrographs of the transversal cross-section of the composites obtained by casting with 5, 10 and 15 wt% of PHB. The presence of PHB was observed in the upper surface of all composites and specifically in the composite with 15 wt% of PHB, it was observed in other internal zones of the paperboard at a low proportion.

In the case of bilayer composites obtained by compression molding, the upper face was attributed to the surface of PHB layer and the lower face, to the surface of the paperboard. Figure 3a and b present the spectra of upper and lower faces of composites obtained by compression molding, respectively. The hydroxyl groups of the cellulose present an absorption peak at 3460 cm^{-1}. Additionally, ester carbonyl group of PHB absorbed at the wavenumber 1755 cm^{-1}, as previously mentioned (Cyras et al. 2009). It was observed that the upper face of the samples present similar spectrum to the typical one of PHB, without contribution of paperboard spectrum (Fig. 3a). At the same time, lower face spectrum showed the same spectrum of paperboard (Fig. 3b). These observations are due to the formation of a continuous PHB coating that covers all the paperboard surface without diffusing through the paperboard layer, indicating greater efficiency of this technique respect to casting (Seoane et al. 2015). FTIR observations were confirmed by SEM, Fig. 4. Micrographs of samples with 15 wt% of PHB weight showed a well differentiated PHB layer with 0.1 mm of average thickness.

Melting temperature (T_m) and crystallinity degree (Xc) of the PHB layer of the composites were determined by DSC. Figure 5a and b present the recorded DSC curves of composites with different PHB contents obtained by casting and compression molding, respectively. The average values of T_m and Xc are shown in Table 1, reporting the highest T_m in the cases with more than one melting peak. A slight difference between T_m values of composites obtained by both techniques was observed, being greater those of compressed composites. This observation could be related to higher perfection and sizes of the crystal due to their reorganization at high temperatures during processing. Bilayer composites obtained by casting presented double melting peaks (Fig. 5a), derived from melting-recrystallization-melting process of the PHB crystals upon heating (Gunaratne et al. 2004). This behavior indicates a great imperfection degree of crystals in these composites (Pearce and Marchessault 1994). Further, PHB in the composites obtained by casting showed lesser Xc than the neat PHB film obtained by the same processing method (55.4%). This result could be because PHB diffuses through paperboard fibers and then, crystallization of PHB is hindered. In addition, Xc was increased with PHB content in the composites. When PHB percentage is 15 wt%, there is enough amount of PHB to form a layer that cover paperboard surface and then, PHB can crystallize without difficulty, reaching a crystalline degree value close to that of neat PHB film.

In the case of compressed composites (Fig. 5b), Xc presented no significant change with the PHB weight until a percentage of 15 wt%, but these values were lesser than the composite with 20 wt% of PHB and the compressed PHB film. These could be due to the effect of paperboard layer on PHB crystallization with low PHB percentage up 15 wt% that hinders crystals growth.

The influence of different percentages of PHB and the processing method in the thermal degradation of the bilayer materials were studied by means of TGA tests. The derivative of the mass loss curves versus temperature (DTG) of each bilayer obtained by both processing techniques and the starting materials are

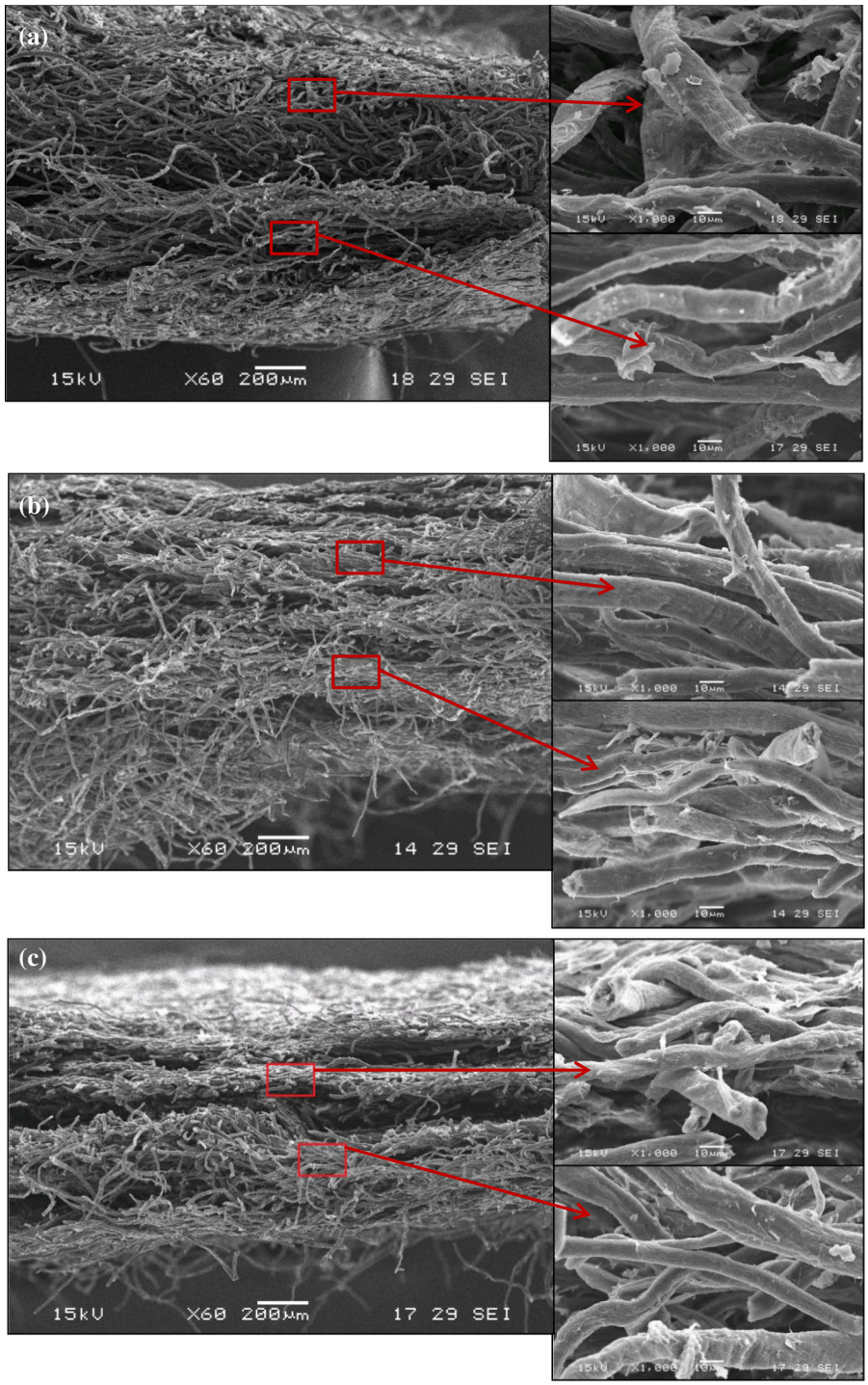

Fig. 2 SEM micrographs of the bilayer composite with **a** 5 wt%, **b** 10 wt% and **c** 15 wt% of PHB content obtained by casting. The upper surface in each image is where PHB was poured

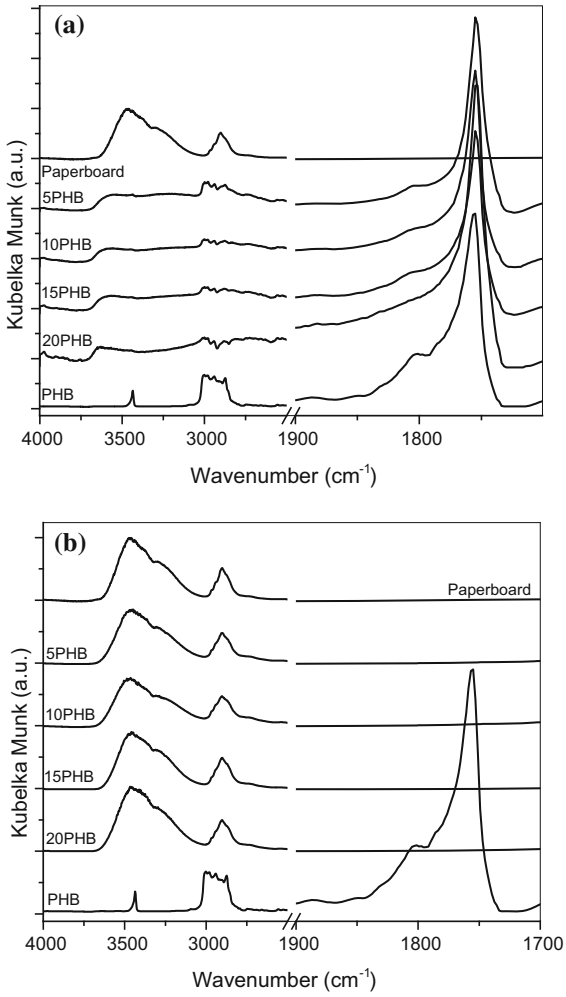

Fig. 3 Normalized FTIR spectra (DRIFT) of **a** upper face and **b** lower face of bilayer composites with different coating percentage obtained by compression molding

shown in Fig. 6. In the DTG curves of each composite, three peaks can be distinguished. The first peak occurred at around 100 °C, which correspond to the evaporation of physically adsorbed and hydrogen bond linked water molecules. This peak was not observed in the DTG curve of the PHB film, indicating that the polymer did not adsorb water. Then, the bilayer composites and the paperboard showed a similar area peak, due to the similar water amount absorbed by the cellulose. The other peaks correspond to the degradation of each layer, being well differentiable both temperature ranges. DTG curves of bilayer composites obtained by casting are presented in Fig. 6a. It was observed that PHB layer degraded at lower temperatures than the pristine film, while the stability of the paperboard layer remained constant. This could be due to the lower crystallinity degree of the PHB in the layer than in the pure film.

DTG curves of the pristine PHB films obtained by casting and compression molding are compared in Fig. 6b. The compressed PHB sample showed higher degradation range temperature, in concordance with the higher crystals ordering, as it was observed by DSC. In addition, DTG curves of bilayer composites obtained by compression molding are also presented in Fig. 6b. It was observed that the thermal stability of the different PHB layers were lower than that of the pristine polymer film, while the paperboard layer did not present alteration. The thermal behavior of the PHB layer can be related to the degree of crystallinity and the crystals ordering of the polymer in the layer. Also, thermal stability of bilayer materials obtained by both processing was slightly increased with the PHB content, according to the PHB crystallinity in each composite.

The mechanical properties of the composites were determined by uniaxial tensile tests. Figure 7a and b show the stress–strain curves of the bilayer composites obtained by casting and compression molding, respectively. In Fig. 8, Young's modulus (E), maximum tensile strength (σ_m) and maximum elongation (ε_m) values of the composites are plotted against the PHB content and the processing technique. The mechanical behavior of bilayer composites showed differences according to the obtaining method. The composites obtained by casting (Fig. 7a) showed a stress–strain curve similar to that of the paperboard, reaching the highest deformation degree and superior σ_m and E values when PHB content was greater than 15 wt%. Further, it was observed that the modulus increased with the percentage of PHB, providing rigidity to the composite. This mechanical behavior responds to the pulling of the cellulose fibers of the paperboard, influenced by PHB-paperboard interface which is the area that supports the applied force (D'Amico et al. 2012). That was corroborated by SEM of the tensile fracture cross-section of the composites obtained by casting (Fig. 9).

In the case of the compression molded composites, they presented higher E and σ_m values than composites obtained by casting, due to the paperboard cellulose fibers compression and the formation of a continuous PHB layer that covered paperboard

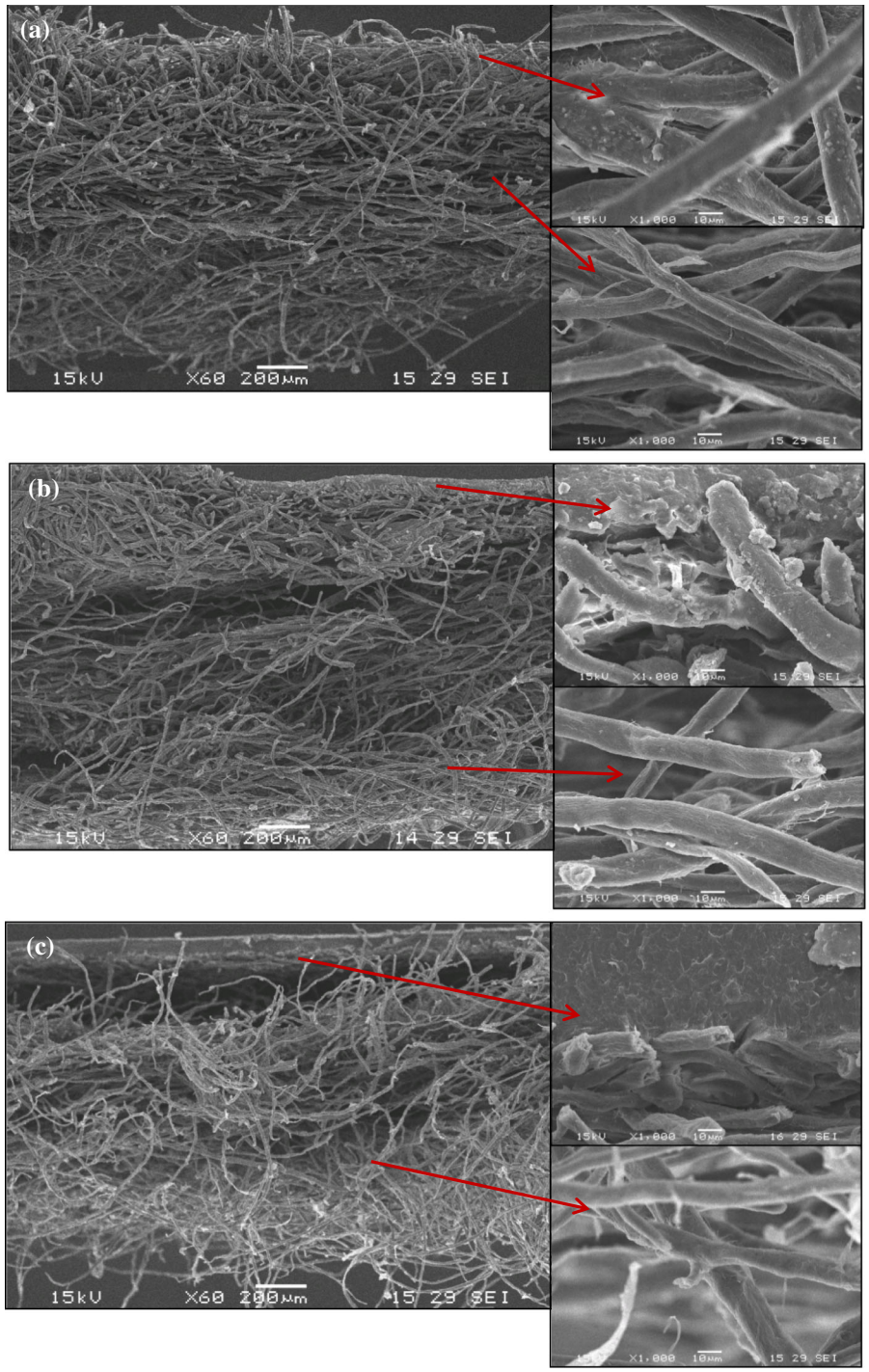

Fig. 4 SEM micrographs of bilayer composite with **a** 5 wt%, **b** 10 wt% and **c** 15 wt% of PHB content obtained by compression molding. The upper surface in each image corresponds to the PHB layer

surface. The interface PHB-paperboard resists the applied forces and restricts the cellulose fibers movement in the paperboard layer, limiting the final deformation of the samples (Cyras et al. 2009). Figure 10 shows the FE-SEM micrograph of the cross-section of a tensile tested sample with 15 wt%

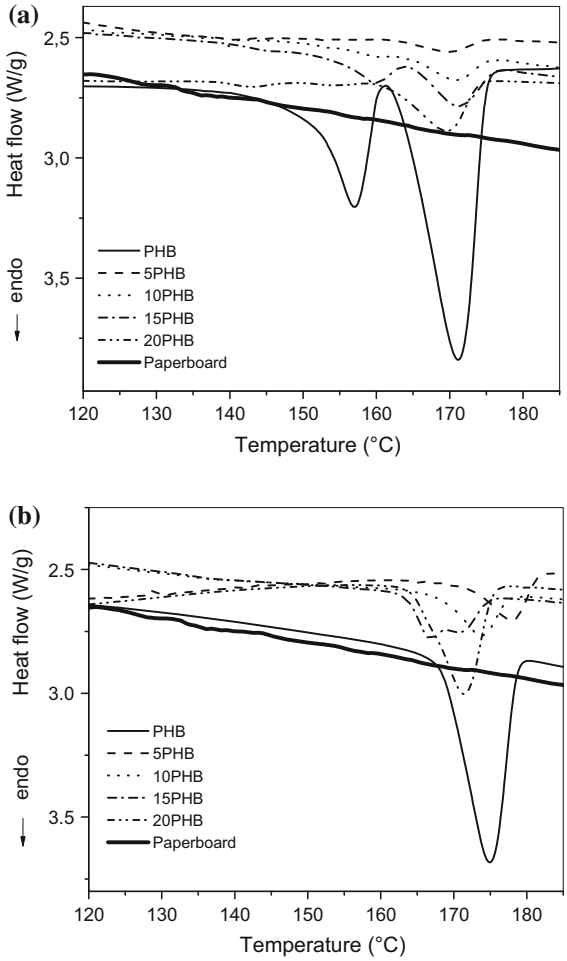

Fig. 5 DSC curves of bilayer composites obtained by: **a** casting and **b** compression molding

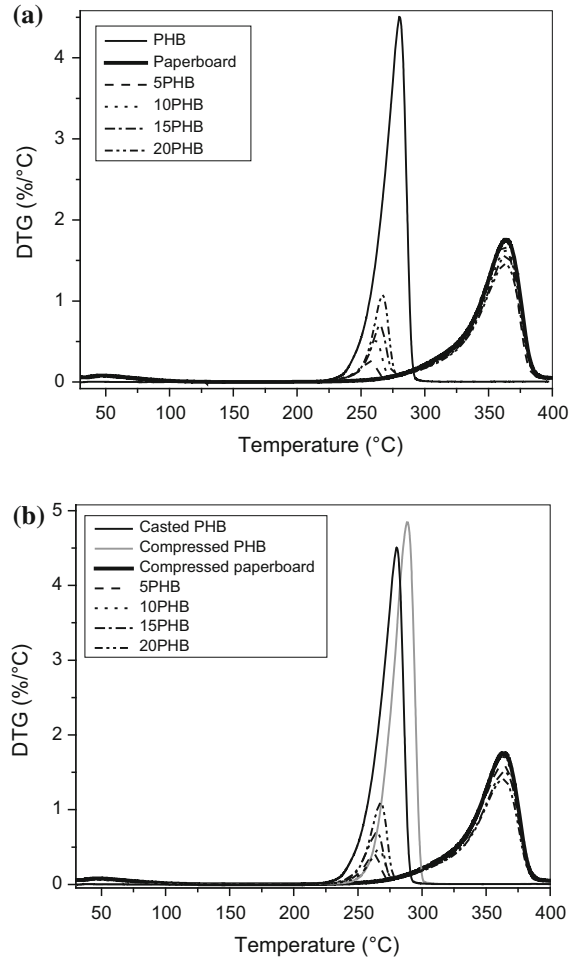

Fig. 6 DTG curves of the samples obtained by: **a** casting and **b** compression molding

Table 1 Xc and T_m average values of PHB in the materials obtained by both processing methods

Processing method	Material	T_m (°C)	Xc (%)
Casting	PHB	171.0 ± 0.5	55.4 ± 0.5
	5PHB	169.2 ± 0.5	31.0 ± 2.0
	10PHB	170.5 ± 0.6	38.0 ± 5.0
	15PHB	170.8 ± 0.5	43.0 ± 5.0
	20PHB	169.9 ± 0.3	47.0 ± 4.0
Compression molding	PHB	174.8 ± 0.1	56.0 ± 4.0
	5PHB	175.0 ± 4.0	38.0 ± 4.0
	10PHB	173.0 ± 4.0	40.0 ± 4.0
	15PHB	171.0 ± 1.0	42.0 ± 4.0
	20PHB	172.0 ± 2.0	59.0 ± 3.0

of PHB, where the continuous layer shown corresponds to PHB. The restriction of cellulose fibers movement by the PHB layer and the peeling of cellulose fibers in the interface were verified by FE-SEM.

Water vapor permeability tests of composites were performed to analyze this property as a function of the PHB content, Fig. 11. It was observed that the bilayer films obtained by casting presented similar permeation to the paperboard. This result is in concordance with the fact that PHB had penetrated into the paperboard layer, being an inefficient barrier to vapor diffusion. In contrast, the permeation of the compressed bilayer films was reduced with the increase of the PHB proportion due to the formation of the PHB layer on the paperboard surface. In addition, a smaller variation

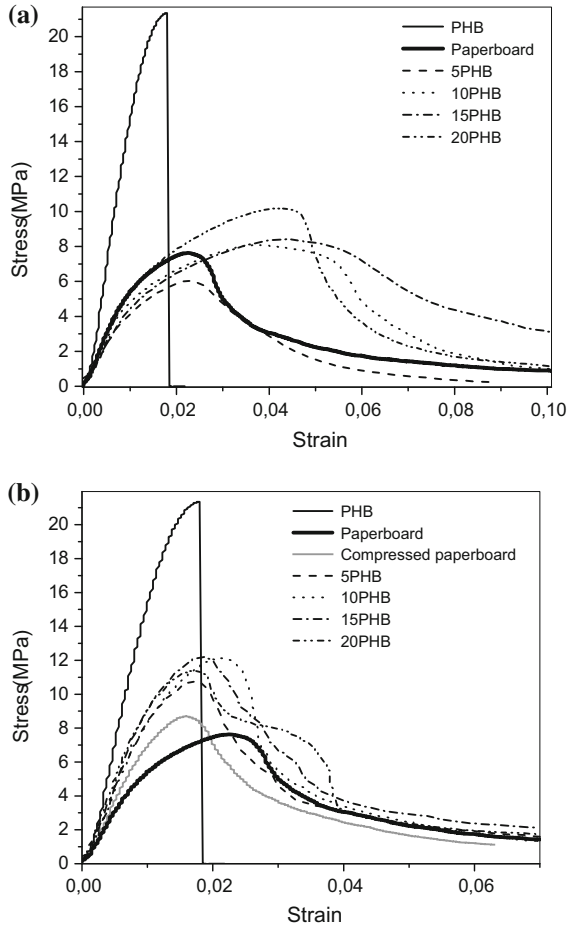

Fig. 7 Strain–stress curves of the bilayer composites obtained by: **a** casting and **b** compression molding

in barrier capacity was observed between compressed composites with 15 and 20 wt% of PHB. This could prove that when the percentage is greater than 15 wt%, the PHB amount is sufficient to entirely cover the paperboard surface, as it was observed by DSC, favoring permeability reduction.

Based on the previous materials characterization, compression molding and 15 wt% of PHB was selected to obtain bilayer films with the addition of cellulose nanoparticles into the polymer layer. It was proved that these technique and percentage of PHB ensure the formation of a continuous layer of polymer covering the paperboard surface and providing suitable mechanical properties and low permeability to be used for packaging. Then, in order to improve the properties of that bilayer material, including the adhesion between the layers, nanocellulose was added to the PHB layer.

Bilayer composites of PHB with CNC and paperboard

Bilayer composites based on nanoreinforced PHB with 4 wt% of CNC and paperboard was obtained by compression molding (15PHB/4CNC). This percentage of nanoparticles was studied for evaluating the effect of this nanoparticle on the bilayer composite properties. Melting properties of the PHB layer of this composite were determined by DSC in order to determine the influence of the CNC on the thermal properties of the PHB. T_m and Xc of this composite resulted (175 ± 1) °C and (66 ± 5)%, respectively. The PHB layer with CNC in the bilayer composites had higher T_m value than 15PHB (Table 1). In addition, Xc was increased with the incorporation of CNC in the formulation. In a previous work, it was observed that CNC act as a good nucleating agent of PHB and the addition of CNC to the PHB matrix favors high ordered crystals of PHB during casting (Seoane et al. 2017). Then, T_m value increment agrees with the crystals rearrangement at high temperatures in the compression process, obtaining greater crystals order and higher crystallinity.

Thermal stability of the bilayer films with CNC was analyzed by TGA and its weight loss curve is presented in Fig. 12. It was observed that the addition of CNC did not increase water adsorption percentage, indicating that CNC was totally immersed into the PHB matrix. Moreover, degradation temperature range of each layer in the composites remained constant with the addition of CNC due to the low added percentage and the system morphology.

Crystalline structure of the bilayer composites was studied by XRD, analyzing both films faces. PHB polymer crystallizes in an orthorhombic unit cell (α-form crystals) under common conditions such as melt, cold or solution crystallization (Cornibert and Marchessault 1972; Wang and Tashiro 2016). The typical X-ray diffraction pattern of the α-form PHB presents peaks at 13.4°, 16.8°, 21.5° and 22.3° of 2θ, corresponding to the planes (020), (110), (101) and (111) (Ten et al. 2012). However, another diffraction peak appeared at 20° in the molded PHB films patterns, which is related to metastable crystals with a "zigzag" conformation (β-form crystals) formed by

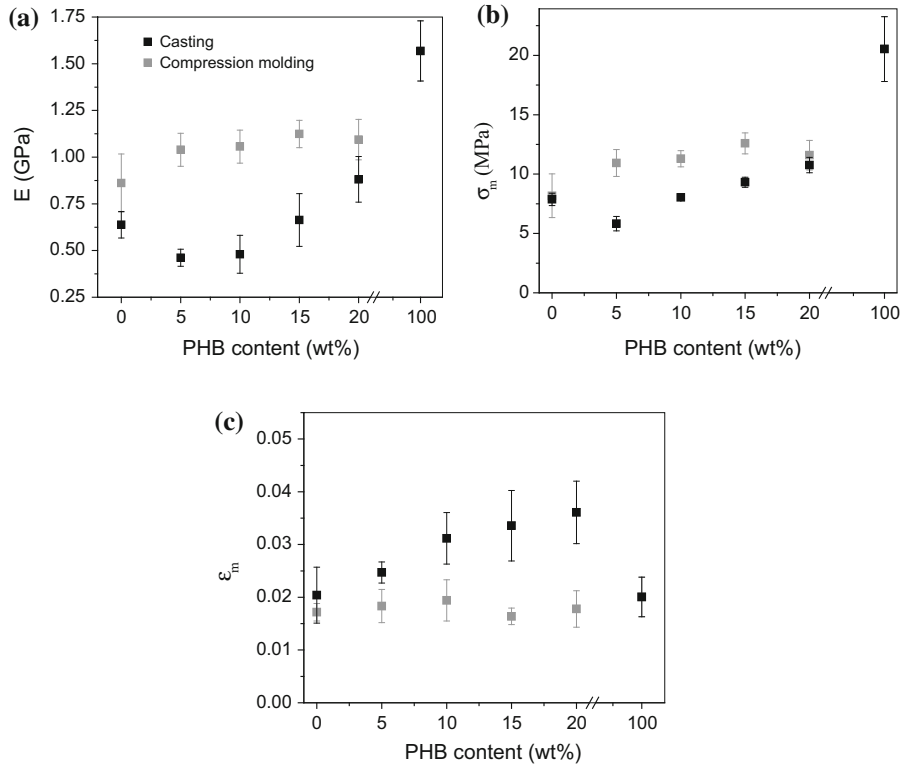

Fig. 8 E (**a**), σ_m (**b**) and ε_m (**c**) values of bilayer composites as a function of PHB content and the processing technique

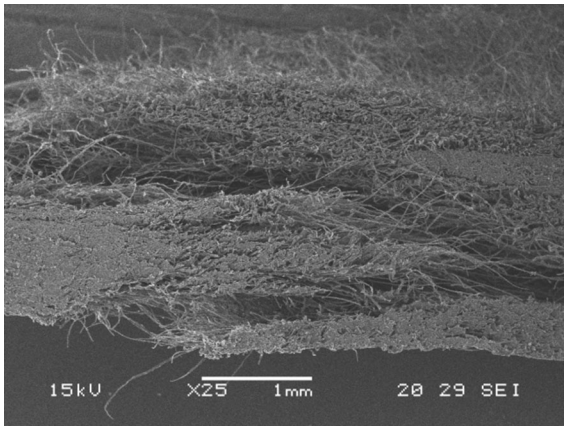

Fig. 9 SEM micrograph of tensile fracture cross-section of a bilayer composite with 15 wt% of PHB obtained by casting, where the upper zone with lower density corresponds to paperboard and the another zone corresponds to PHB

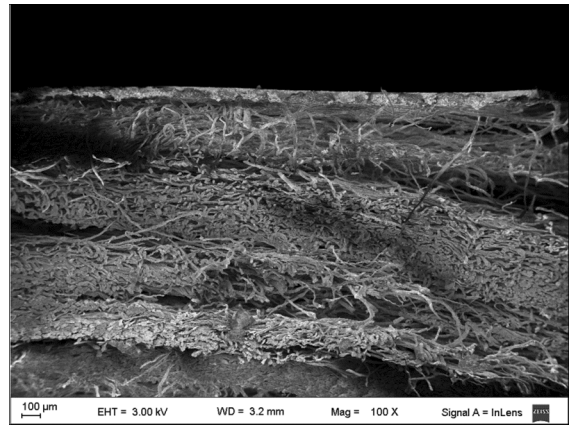

Fig. 10 FE-SEM micrograph of tensile fracture cross-section of a bilayer composite with 15 wt% of PHB obtained by compression molding, where the upper zone corresponds to the PHB layer and the lower zone corresponds to the paperboard

a molecular stretching of the amorphous region between the lamellae of α-form crystals (Wang et al. 2008; Pan and Inoue 2009; Mottin et al. 2016). Regarding the paperboard, it shows the characteristic crystalline peaks of cellulose I, that are located at 14.5°, 16.4° and 22.5° of 2θ. The upper and lower face spectra of the compression molded bilayer samples (15PHB and 15PHB/4CNC) are shown in Figs. 13 and 14, respectively. In Fig. 13, it was included the spectra of the native PHB films obtained by casting and compression molding with comparison purpose. It was observed that compressed film spectrum presented

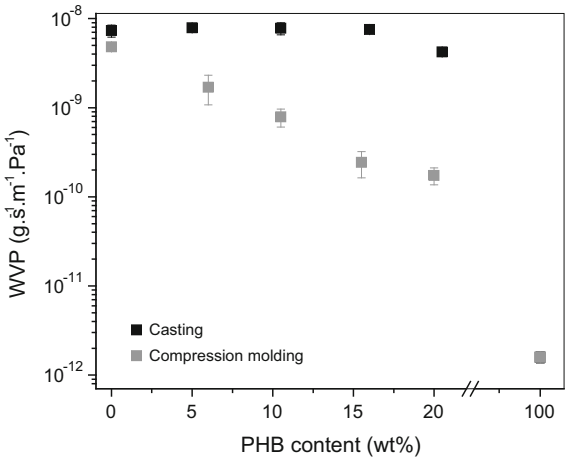

Fig. 11 WVP values of bilayer composites as a function of PHB content and the processing technique

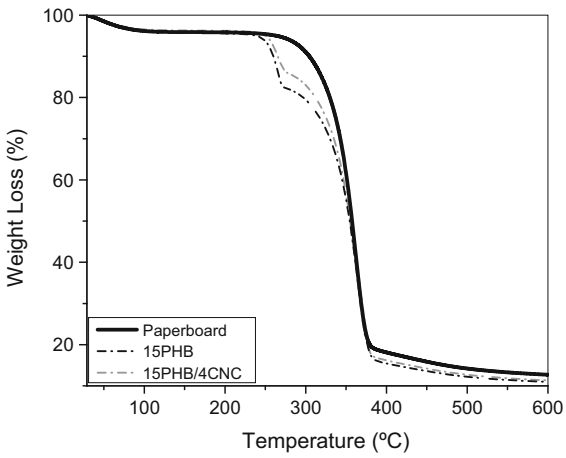

Fig. 12 Weight loss curves of molded samples

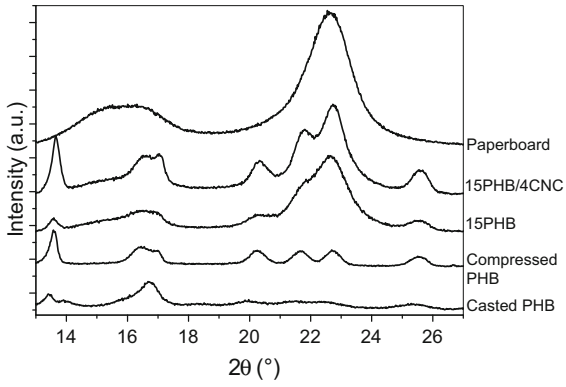

Fig. 13 XRD spectra of PHB films obtained by casting and compression molding, paperboard and coated-paperboard upper face samples (15PHB and 15PHB/4CNC)

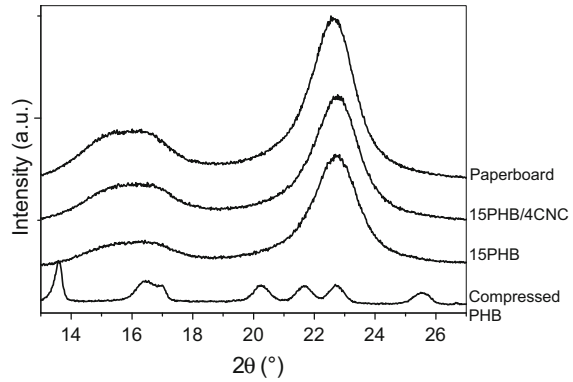

Fig. 14 XRD spectra of compressed PHB, paperboard and coated-paperboard lower face samples (15PHB and 15PHB/4CNC)

more defined peaks than the spectrum of the film obtained by casting. This observation responds to the higher crystal ordering of compressed samples. Another observation is the intensity increment of the peak located at 20°, attributed to the PHB β-form crystals. It was inferred that the β-form crystals were obtained from a uniaxial stretching process occurred during the compression molding (Gong et al. 2015; Mottin et al. 2016). Regarding the compressed bilayer composites, the spectra of the corresponding upper faces presented the characteristics peaks of PHB and cellulose overlapped because of the XRD penetration depth is higher than the coated-layer thickness (Cyras et al. 2009). Further, the crystalline peaks attributed to PHB presented greater intensity when CNC were added in the coating formulation. This result indicates the highest crystalline degree and crystal ordering of this composite and verifies DSC observations. Moreover, the lower faces spectra of the compressed bilayer films presented the same pattern of the paperboard (Fig. 14), indicating PHB absence at this film side.

Tensile and permeation tests were performed to evaluate the effect of CNC on the mechanical and barrier properties of the bilayer composite. The average values of E, σ_m, ε_m and WVP of the samples are presented in Table 2. The bilayer composite with CNC (15PHB4CNC) presented a similar mechanical behavior to 15PHB and a significant reduction of water permeation by one order of magnitude. These results may be due to a higher crystallinity degree (as it was observed by DSC and XRD) and higher interfacial interaction induced by the addition of CNC that ensure the adhesion between the paperboard and the PHB

Table 2 E, σ_m, ε_m and WVP average values of compressed paperboard and coated-paperboard

Sample	E (MPa)	σ_m (MPa)	ε_m	WVP $\times$ 10^{11} (g s^{-1} m^{-1} Pa^{-1})
Paperboard	860 ± 150	8.5 ± 1.6	0.015 ± 0.003	482 ± 16
15PHB	1120 ± 70	12.6 ± 0.9	0.016 ± 0.002	22 ± 8
15PHB/4CNC	1100 ± 130	10.4 ± 1.3	0.017 ± 0.003	3 ± 1

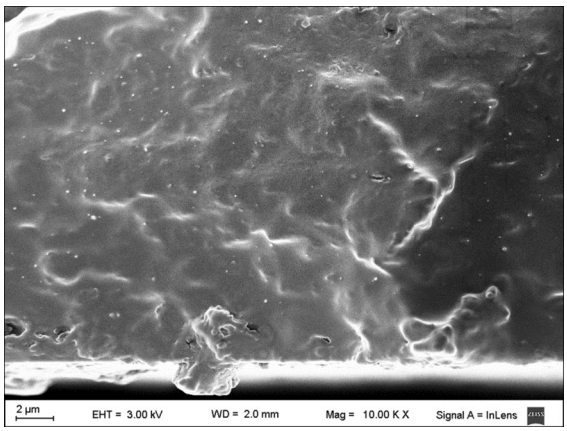

Fig. 15 FE-SEM micrograph of the fracture surface of a film based on PHB with 4 wt% of CNC

layers. Dispersion of the nanoparticles in the polymeric matrix is an important factor that favors the interfacial interaction increment. This feature was determined by FE-SEM, analyzing the fracture surface of a PHB based film with 4 wt% of CNC (Fig. 15). In the micrograph, the filler could be identified as white particles into the dark matrix of PHB (Azizi Samir et al. 2005). The sample presented good dispersion of the nanoparticles, as it was concluded in a previous work (Seoane et al. 2017). Further, the addition of a dispersed nanofiller could increase the tortuosity of the water pathway through the polymeric matrix, reducing the permeation of the composite (Rastogi and Samyn 2015). The barrier property improvement due to the addition of CNC was already observed in several

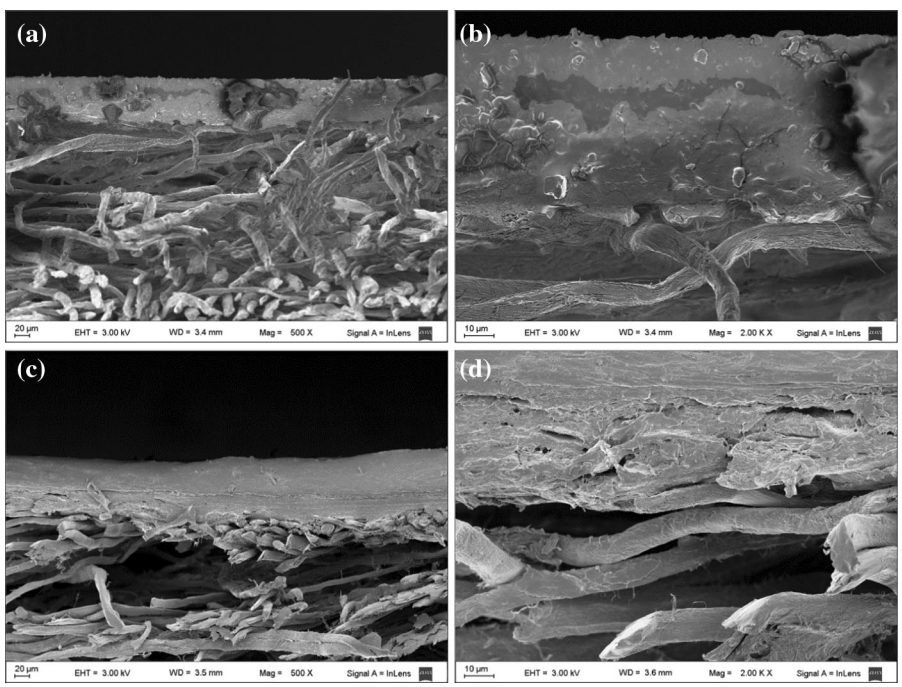

Fig. 16 FE-SEM micrographs of tensile fracture cross-section of bilayer composites obtained by compression molding: **a** and **b** 15PHB, **c** and **d** 15PHB/4CNC, with different magnification. The upper zone corresponds to the PHB-based layer and the lower zone corresponds to the paperboard

works (Brinchi et al. 2013; de Carvalho et al. 2016; Seoane et al. 2016).

The interfacial region was characterized by FE-SEM to analyze the layers adhesion. The images of the fractured bilayer samples cross-section are shown in Fig. 16, focusing on the interfacial region. In the micrograph of the sample 15PHB, it was observed several fibers that were peeled from the coating interface. The bilayer composite with CNC presented a higher amount of fibers that remained adhered to the PHB coating or were torn after be peeled. In addition, the coating based on PHB and CNC presented high deformation around the fracture. Because of these, higher interfacial interaction between the coating and the cellulose fibers of the paperboard were observed with the addition of the hydrophilic nanoparticles. Then, this interaction improvement could contribute to the reduction of the water permeation through the nanocomposite.

Conclusions

Bilayer composites bases on PHB and cellulose paperboard with different coating proportions were obtained by means of two different process: casting and compression molding. Compression molding was selected as the most effective technique to achieve a continuous layer of PHB covering the surface of the paperboard. In addition, this method is most appropriate for its eventual industrial application, taking advantage of the thermoplasticity that this biopolymer presents. The selected PHB/paperboard proportion was 15 wt% as it corresponds to the minimum amount of PHB that ensures full paperboard coating, reaching higher Young's modulus, maximum tensile strength and lesser water vapor permeability than the other studied materials.

A bilayer nanocomposite was then produced according to the selected method and PHB proportion. The nanocomposite film, used as paperboard coating, presented good dispersion of the nanoparticles, being an important factor that influences the thermal, mechanical and barrier properties of the composite and also, affects the interfacial interaction degree between the coating layer and the paperboard.

Crystallinity degree and crystal ordering of PHB in the bilayer composite were increased when CNC was added (15PHB/4CNC). In addition, a higher interfacial interaction was induced, ensuring the adhesion between the hydrophilic paperboard and the hydrophobic PHB layer, as it was observed by FE-SEM. Therefore, the addition of a hydrophilic nanoparticle into the hydrophobic matrix promotes hydrophilic character of the PHB based nanocomposite.

Bilayer nanocomposites maintain good mechanical properties, presenting the delamination behavior characteristic of the paperboard with higher modulus and maximum tension strength values. Additionally, this sample showed a significant reduction on water permeability compared to the permeability of the paperboard or the coated-paperboard with neat PHB. Mechanical and barrier properties resulted in agreement with the increment of the crystallinity degree, the interfacial interaction and the tortuosity of the diffusional pathway, due to the addition of CNC in the PHB based coating formulation.

According to the results obtained, PHB has the potential to replace non-renewable polymers as eco-friendly material for paperboard coating application. Furthermore, the inclusion of CNC into the coating formulation overcomes water sensibility of the cellulose paperboard, indicating that this material could be used for packaging.

Acknowledgments The authors acknowledge the financial support of CONICET (PIP 0527) and Universidad Nacional de Mar del Plata.

References

Andersson C (2008) New ways to enhance the functionality of paperboard by surface treatment—a review. Packag Technol Sci 21:339–373. https://doi.org/10.1002/pts.823

Arrieta MP, Samper MD, Aldas M, López J (2017) On the use of PLA–PHB blends for sustainable food packaging applications. Materials (Basel) 10:1–26. https://doi.org/10.3390/ma10091008

Azizi Samir M, Alloin F, Dufresne A (2005) Review of recent research into cellulosic whisker, their properties and their application in nanocomposites field. Biomacromol 6:612–626

Barham PJ, Keller A, Otun EL, Holmes PA (1984) Crystallization and morphology of a bacterial thermoplastic: poly-3-hydroxybutyrate. J Mater Sci 19:2781–2794. https://doi.org/10.1007/BF01026954

Brinchi L, Cotana F, Fortunati E, Kenny JM (2013) Production of nanocrystalline cellulose from lignocellulosic biomass: technology and applications. Carbohydr Polym

94:154–169. https://doi.org/10.1016/j.carbpol.2013.01.033

Cornibert J, Marchessault RH (1972) Physical properties of poly-β-hydroxybutyrate. J Mol Biol 71:735–756. https://doi.org/10.1016/S0022-2836(72)80035-4

Cyras VP, Commisso MS, Mauri AN, Vázquez A (2007) Biodegradable double-layer films based on biological resources: polyhydroxybutyrate and cellulose. J Appl Polym Sci 106:749–756. https://doi.org/10.1002/app.26663

Cyras VP, Commisso MS, Vázquez A (2009) Biocomposites based on renewable resource: acetylated and non acetylated cellulose cardboard coated with polyhydroxybutyrate. Polymer (Guildf) 50:6274–6280. https://doi.org/10.1016/j.polymer.2009.10.065

D'Amico DA, Manfredi LB, Cyras VP (2012) Relationship between thermal properties, morphology, and crystallinity of nanocomposites based on polyhydroxybutyrate. J Appl Polym Sci 123:20–208. https://doi.org/10.1002/app.26663

de Carvalho KCC, Montoro SR, Cioffi MOH, Voorwald HJC (2016) Polyhydroxyalkanoates and their nanobiocomposites with cellulose nanocrystals. In: Thomas S, Shanks R, Chandrasekharakurup S (eds) Design and applications of nanostructured polymer blends and nanocomposite systems. Elsevier, Oxford, pp 261–285

Desobry S, Arab-Tehrany E (2014) Diffusion barrier layers for edible food packaging. In: Comprehensive materials processing. Elsevier, pp 499–518

Farmer N (2013) The future: global trends and analysis for the international packaging market in relation to the speed of impact of packaging innovation and likely material changes. In: Trends in packaging of food, beverages and other fast-moving consumer goods (FMCG). Elsevier, pp 288–312

Gong L, Chase DB, Noda I et al (2015) Discovery of β-form crystal structure in electrospun poly[(R)-3-hydroxybutyrate-co-(R)-3-hydroxyhexanoate] (PHBHx) nanofibers: from fiber mats to single fibers. Macromolecules 48:6197–6205. https://doi.org/10.1021/acs.macromol.5b00638

Gunaratne LMWK, Shanks RA, Amarasinghe G (2004) Thermal history effects on crystallisation and melting of poly(3-hydroxybutyrate). Thermochim Acta 423:127–135. https://doi.org/10.1016/j.tca.2004.05.003

Johansson C, Bras J, Mondragon I et al (2012) Renewable fibers and bio-based materials for packaging applications—a review of recent developments. BioResources 7:2506–2552. https://doi.org/10.15376/biores.7.2.2506-2552

Kontominas MG (2010) Packaging and the shelf life of milk. In: Robertson GL (ed) Food packaging and shelf life—a practical guide. CRC Press, Boca Raton, pp 81–102

Mekonnen T, Mussone P, Khalil H, Bressler D (2013) Progress in bio-based plastics and plasticizing modifications. J Mater Chem A 1:13379–13398. https://doi.org/10.1039/c3ta12555f

Morán JI, Alvarez VA, Cyras VP, Vázquez A (2008) Extraction of cellulose and preparation of nanocellulose from sisal fibers. Cellulose 15:149–159. https://doi.org/10.1007/s10570-007-9145-9

Mottin AC, Ayres E, Eliane A et al (2016) What changes in poly (3-hydroxybutyrate) (PHB) when processed as electrospun nanofibers or thermo-compression molded film? Mater Res 19:57–66

Njuguna J, Wambua P, Pielichowski K, Kayvantash K (2011) Natural fibre-reinforced polymer composites and nanocomposites for automotive applications. Cellulose fibers: bio-and nano-polymer composites. Springer, Berlin, pp 661–700

Pan P, Inoue Y (2009) Polymorphism and isomorphism in biodegradable polyesters. Prog Polym Sci 34:605–640. https://doi.org/10.1016/j.progpolymsci.2009.01.003

Pearce R, Marchessault R (1994) Multiple melting in blends of isotactic and atactic poly(β-hydroxybutyrate). Polymer (Guildf) 35:3990–3997. https://doi.org/10.1016/0032-3861(94)90285-2

Peelman N, Ragaert P, De Meulenaer B et al (2013) Application of bioplastics for food packaging. Trends Food Sci Technol 32:128–141. https://doi.org/10.1016/j.tifs.2013.06.003

Plackett D, Vázquez A (2004) Natural polymer sources. In: Baillie C (ed) Green composites. Woodhead Publishing Limited, Cambridge, pp 123–153

Puglia D, Fortunati E, D'Amico DA et al (2016) Influence of processing conditions on morphological, thermal and degradative behavior of nanocomposites based on plasticized poly(3-hydroxybutyrate) and organo-modified clay. J Polym Environ 24:12–22. https://doi.org/10.1007/s10924-015-0744-5

Rastogi V, Samyn P (2015) Bio-based coatings for paper applications. Coatings 5:887–930. https://doi.org/10.3390/coatings5040887

Robertson GL (2013) Paper and paper-based packaging materials. In: Food packaging principles and practice. CRC Press, pp 167–188

Saxena M, Pappu A, Haque R, Sharma A (2011) Sisal fiber based polymer composites and their applications. Cellulose fibers: bio- and nano-polymer composites. Springer, Berlin, pp 589–659

Seoane IT, Manfredi LB, Cyras VP (2015) Properties and processing relationship of polyhydroxybutyrate and cellulose biocomposites. Procedia Mater Sci 8:807–813. https://doi.org/10.1016/j.mspro.2015.04.139

Seoane IT, Fortunati E, Puglia D et al (2016) Development and characterization of bionanocomposites based on poly (3-hydroxybutyrate) and cellulose nanocrystals for packaging applications. Polym Int. https://doi.org/10.1002/pi.5150

Seoane IT, Cerrutti P, Vazquez A et al (2017) Polyhydroxybutyrate-based nanocomposites with cellulose nanocrystals and bacterial cellulose. J Polym Environ 25:586–598. https://doi.org/10.1007/s10924-016-0838-8

Siracusa V, Rocculi P, Romani S, Rosa MD (2008) Biodegradable polymers for food packaging: a review. Trends Food Sci Technol 19:634–643. https://doi.org/10.1016/j.tifs.2008.07.003

Ten E, Jiang L, Wolcott MP (2012) Crystallization kinetics of poly(3-hydroxybutyrate-co-3-hydroxyvalerate)/cellulose nanowhiskers composites. Carbohydr Polym 90:541–550. https://doi.org/10.1016/j.carbpol.2012.05.076

Wang H, Tashiro K (2016) Reinvestigation of crystal structure and intermolecular interactions of biodegradable poly(3-hydroxybutyrate) α-form and the prediction of its mechanical property. Macromolecules 49:581–594. https://doi.org/10.1021/acs.macromol.5b02310

Wang C, Hsu C-H, Hwang I-H (2008) Scaling laws and internal structure for characterizing electrospun poly[(R)-3-

hydroxybutyrate] fibers. Polymer (Guildf) 49:4188–4195. https://doi.org/10.1016/j.polymer.2008.07.033

Yu H, Yan C, Yao J (2014) Fully biodegradable food packaging materials based on functionalized cellulose nanocrystals/poly(3-hydroxybutyrate-co-3-hydroxyvalerate) nanocomposites. RSC Adv 4:59792–59802. https://doi.org/10.1039/C4RA12691B